

Gas and dust in NGC 7469: sub-mm imaging and CO J=3–2

Padeli P. Papadopoulos¹

and

Michael L. Allen ²

Received _____; accepted _____

¹Sterrewacht Leiden, P. O. Box 9513, 2300 RA Leiden, The Netherlands

²Department of Astronomy, University of Toronto, 60 St. George street, Toronto,
ON M5S-3H8, Canada

ABSTRACT

We present sensitive sub-mm imaging of the Seyfert 1 galaxy NGC 7469 at 850 μm and 450 μm with the Submillimetre Common User Bolometer Array (SCUBA) on the James Clerk Maxwell Telescope (JCMT) and ^{12}CO J=3–2 line observations of its central starbursting region. The global dust spectrum, as constrained by the new set of sub-mm data and available 1.30 mm and IRAS 100 μm , 60 μm data reveals a dominant warm dust component with a temperature of $T_d \sim 35$ K and a global molecular gas-to-dust ratio $M(\text{H}_2)/M_d \sim 600$. Including the atomic gas component yields a total gas-to-dust ratio of ~ 830 . Such high values are typical for IR-bright spirals and in order to reconcile them with the significantly lower ratio of ~ 100 obtained for the Milky Way a cold dust reservoir, inconspicuous at FIR wavelengths, is usually postulated. However, while there is good evidence for the presence of cold gas/dust in NGC 7469 beyond its central region, our 450 μm map and available interferometric ^{12}CO J=1–0 maps show the bright sub-mm/CO emission confined in the inner ~ 2.5 kpc, where a high ^{12}CO (J=3–2)/(J=1–0) ratio ($\sim 0.85 - 1.0$) is measured. This is consistent with molecular gas at $T_{\text{kin}} \gtrsim 30\text{K}$, suggesting that the bulk of the ISM in the starburst center of NGC 7469 is warm. Nevertheless the corresponding total gas-to-dust ratio there remains high, of the order of ~ 500 . We argue that, rather than unaccounted cold dust mass, this high ratio suggests an overestimate of $M(\text{H}_2)$ from its associated ^{12}CO J=1–0 line luminosity by a factor of ~ 5 when a Milky Way value for this conversion is used. Finally the diffuse cold gas and dust that is the likely source of the observed faint extended 450 μm and ^{12}CO J=1–0 emission has an estimated total gas-to-dust ratio of $\sim 50 - 160$, closer to the Galactic value.

Subject headings: galaxies: individual (NGC 7469)—galaxies: ISM—galaxies: Seyfert—galaxies: starburst

1. Introduction

The role of molecular gas as the fuel of both starburst activity and an Active Galactic Nucleus (AGN) is now well established. In Seyfert galaxies such gas is found on scales ranging from the inner $\sim 1 - 2$ kpc “feeding” an intense circumnuclear starburst down to $L \lesssim 100$ pc from the AGN, where in the form of a geometrically thick torus obscures the active nucleus along certain viewing angles thus creating the difference between type 2 and type 1 Seyferts (Miller & Antonucci 1983; Krolik 1990 and references therein).

Estimates of molecular gas mass in other galaxies from their velocity-integrated ^{12}CO J=1–0 luminosity L_{CO} (in $\text{K km s}^{-1} \text{ pc}^2$) are based on the so-called conversion factor $X_{\text{CO}} = \text{M}(\text{H}_2)/L_{\text{CO}} \approx 5 \text{ M}_{\odot}(\text{K km s}^{-1} \text{ pc}^2)^{-1}$ (e.g. Solomon & Barrett 1991) whose value is derived from studies of molecular gas in the Galactic disk. Numerous studies quantify the effects of the various physical conditions on this factor (e.g. Bryant & Scoville 1996; Israel 1997). Particularly in the starburst nuclei of very luminous IR galaxies ($L_{\text{FIR}} > 10^{11} L_{\odot}$) these conditions are significantly different than in the disk environment of quiescent spirals like the Milky Way. More specifically in the inner $\sim 1 - 2$ kpc, where a starburst usually occurs, the gas differentiates into two distinct phases (e.g. Aalto et al. 1995) with a warm, diffuse and possibly non self-gravitating phase dominating the ^{12}CO emission. This results in a significant overestimate of H_2 mass from L_{CO} when a Galactic value of X_{CO} is used (Solomon et al. 1997; Downes & Solomon 1998).

The aforementioned conditions are expected in the nuclear region of the SBa Seyfert 1 galaxy NGC 7469 (Arp 298, Mrk 1514), a luminous IR source with $L_{\text{FIR}} \approx 3 \times 10^{11} L_{\odot}$ emanating from a powerful starburst deeply embedded into its $L \sim 1$ kpc circumnuclear region (Wilson et al. 1991; Genzel et al. 1995). High resolution ^{12}CO J=1–0 observations revealed large amounts of molecular gas within this region (Meixner et al. 1990; Tacconi & Genzel 1996) with mass comparable to the dynamical, and there is significant evidence

that application of the standard Galactic conversion factor overestimates $M(\text{H}_2)$ in the circumnuclear starburst of this galaxy (Genzel et al. 1995). In this paper we present sensitive sub-mm imaging of NGC 7469 at 850 μm and 450 μm and ^{12}CO J=3–2 spectroscopy of its central region. Under the assumption of a canonical gas-to-dust ratio of ~ 100 , our results confirm the overestimate of H_2 gas mass when a Galactic value for X_{CO} is used, and demonstrate the significance of CO spectroscopy and sub-mm imaging in offering a better assessment of the molecular gas mass and its average physical conditions.

Throughout this work we adopt $H_0 = 75 \text{ km sec}^{-1} \text{ Mpc}^{-1}$ and $q_0 = 0.5$, which for $cz=4900 \text{ km s}^{-1}$ yields a luminosity distance of $D_L \sim 66 \text{ Mpc}$ for NGC 7469, where $1''$ corresponds to $\sim 310 \text{ pc}$.

2. Observations

The sub-mm observations were made on the nights of 1997 December 3 and 1998 January 15 with the Sub-mm Common User Bolometer Array (SCUBA) at the 15-m James Clerk Maxwell Telescope (JCMT)³. SCUBA is a dual camera system cooled to $\sim 0.1 \text{ K}$ allowing sensitive simultaneous observations with two arrays. The short-wavelength array contains 91 pixels and the long-wavelength array 37 pixels, with approximately the same field of view, namely $\sim 2.3'$. For a description of the instrument see Holland et al. (1998).

We performed dual wavelength imaging at 450 μm and 850 μm using the 64-point jiggle mapping mode that allows Nyquist sampling of the field of view. (Holland et al. 1998). We employed the recommended rapid beam switching at a frequency of $\sim 8 \text{ Hz}$ and

³The JCMT is operated by the Joint Astronomy Center in Hilo, Hawaii on behalf of the parent organizations PPARC in the United Kingdom, the National Research Council of Canada and the The Netherlands Organization for Scientific Research.

a beam throw of $150''$ in azimuth. The pointing and focus were monitored frequently using Uranus and CRL 618, with an expected rms pointing error of $\sim 3''$. All maps of NGC 7469 were “bracketed” by sky-dips that were later used to correct for atmospheric extinction. Conditions were generally excellent for sub-mm observations with typical opacities of $\tau_{850} \sim 0.1 - 0.2$ and $\tau_{450} \sim 0.45 - 0.55$ throughout our runs.

The beam characteristics and calibration gains ($\text{Jy V}^{-1} \text{ beam}^{-1}$) were deduced from an extensive archive of beam maps of Uranus and CRL 618 taken during similar periods as our observations and with a similar beam-throw ($120''$). High S/N beam maps are particularly important for the calibration of $450 \mu\text{m}$ images since the beam shape and the gain can change significantly as the dish thermally relaxes. All jiggle maps were flat-fielded, corrected for atmospheric extinction and edited for bad bolometers/integrations using the standard reduction package SURF (Jenness & Lightfoot 1998). Sky-noise was removed by using the bolometers in the outer ring of the two arrays (Jenness, Lightfoot & Holland 1998) which were assumed “looking” only at sky emission. This is a good assumption for NGC 7469 where most of its ^{12}CO J=1–0 emission (and presumably most of the sub-mm emission from dust) lies within a $\sim 4''$ radius (Tacconi & Genzel 1996, Tacconi et al. 2000).

The gain and beam characteristics at $850 \mu\text{m}$ remained essentially the same throughout the runs. This is further corroborated by the fact that the “raw” peak and integrated intensities of the NGC 7469 images at this wavelength agree to within $\sim 10\%$, which is the expected calibration uncertainty. Hence we co-added all the noise-weighted frames after subtracting a small gradient from one of them, and then scale the final one with the single gain factor of $G_{850} = 290 \text{ Jy Volt}^{-1} \text{ beam}^{-1}$. The deduced beam-width is $\Theta_{\text{HPBW}}^{(850)} \sim 15''$.

The $450 \mu\text{m}$ beam maps revealed substantial gain variations ($\sim 40\%$) between observations taken early in the first shift and the ones taken later on, presumably due to the thermal relaxation of the dish. Thus before co-adding the images of NGC 7469

we scaled them by the appropriate gains of $G_{450} = 1170 \text{ Jy Volt}^{-1} \text{ beam}^{-1}$ and $G_{450} = 780 \text{ Jy Volt}^{-1} \text{ beam}^{-1}$. This scaling brought their peak and integrated intensities in agreement to within $\sim 15\%$, which is comparable to the calibration uncertainty expected at $450 \mu\text{m}$. The average beam-width deduced for this wavelength is $\Theta_{\text{HPBW}}^{(450)} \sim 9''$.

The ^{12}CO J=3–2 line at 345.796 GHz was observed towards the nucleus of NGC 7469 with receiver B3 on 1999 August 6. We used the DAS spectrometer with a bandwidth of 920 MHz ($\sim 800 \text{ km s}^{-1}$), and two independent channels centered on the line. The chop scheme employed was rapid beam switching with a $120''$ azimuthal throw at the recommended frequency of 1 Hz. The HPBW of the telescope beam at this frequency is $\sim 14''$ with a beam efficiency of $\eta_{\text{mb}} = 0.62$ (Matthews 1999). Typical system temperatures were of the order of $T_{\text{sys}} \sim 600 \text{ K}$. After subtracting linear baselines from all spectra their integrated line intensities were found to agree to within $\sim 10\%$, the typical calibration uncertainty for receiver B3. We then co-added all of them to produce the final spectrum.

3. RESULTS

The galaxy is detected as a bright sub-mm source at $850 \mu\text{m}$ where it appears marginally resolved, as well as at $450 \mu\text{m}$ where it clearly shows faint extended emission. We convolved a high-resolution map of ^{12}CO J=1–0 emission (Tacconi et al. 2000) from its original resolution of $\sim 2.5''$ to the resolution of the $450 \mu\text{m}$ map ($\sim 9''$) and show them, together with the $850 \mu\text{m}$ map, in Figure 1.

EDITOR: PLACE FIGURE 1 HERE.

The correspondence between the bright $450 \mu\text{m}$ and ^{12}CO J=1–0 emission is very good, suggesting that they both trace the same ISM material. The high-resolution interferometric

^{12}CO J=1–0 maps (Tacconi & Genzel 1996; Tacconi et al. 2000) show bright emission arising from a region with a diameter of $d \sim 8''$, where an intense starburst is embedded (Wilson et al. 1991), hence the presence of warm gas and dust is expected there. Indeed the central region of NGC 7469, besides hosting an AGN, also harbors several supergiant star formation regions containing numerous ($\text{few} \times 10^4$) OB stars each (Genzel et al. 1995), whose intense UV light and subsequent supernova explosions will warm and disrupt the molecular clouds present. The warm dust of these clouds can easily dominate the global FIR and even the mm/sub-mm emission from this galaxy. In principle the new sub-mm measurements allow for a better evaluation of the dust mass and temperature. Thus in Table 1 we compile them together with available mm and FIR data and use them to model the dust emission SED, shown in Figure 2.

EDITOR: PLACE TABLE 1 HERE

EDITOR: PLACE FIGURE 2 HERE.

The reported mm/sub-mm fluxes at 1.3 mm and $850 \mu\text{m}$ have been corrected for non-dust emission from CO lines, which can be rather significant (see Appendix). The fitted dust temperature and mass are: $T_d \sim 35 \text{ K}$ and $M_d = 2.5 \times 10^7 M_\odot$. It can be seen that a single dust component fits the data rather well, except for wavelengths shortward of $60 \mu\text{m}$ where the hot dust ($\gtrsim 300 \text{ K}$) present in the central region (Cutri et al. 1984) makes a significant contribution to the total flux but contains a negligible fraction ($\leq \text{few} \times 10^{-4}$) of the total dust mass. From the ^{12}CO J=1–0 map obtained by Tacconi et al. (2000), we find a total flux of $S_{\text{CO}} = (275 \pm 30) \text{ Jy km s}^{-1}$, which allows an estimate the global molecular mass from

$$M(\text{H}_2) = 2.45 \times 10^3 X_{\text{CO}} D^2 S_{\text{CO}} \quad (1)$$

where $D=66$ Mpc and $X_{\text{CO}} \sim 5 \text{ M}_\odot (\text{km s}^{-1} \text{ pc}^2)^{-1}$. This yields a mass of $M(\text{H}_2) \approx 1.5 \times 10^{10} \text{ M}_\odot$ and $M(\text{H}_2)/M_d \approx 600$, a typical value for IRAS galaxies (Young et al. 1986; Young et al. 1989; Stark et al. 1986). Including the HI gas mass $M(\text{HI}) = 5.7 \times 10^9 \text{ M}_\odot$ (Mirabel & Wilson 1984) yields a total gas-to-dust ratio of ~ 830 .

The presence of warm and dense molecular gas in the nucleus of NGC 7469 is responsible for the strong ^{12}CO J=3–2 line observed towards it. The high resolution ^{12}CO J=1–0 interferometer map allows for an estimate of the (J=3–2)/(J=1–0) line ratio in the inner $d \sim 8''$ of this galaxy. This is possible since virtually all the bright ^{12}CO J=1–0 emission lies within that region, and hence the ^{12}CO J=3–2 emission with its higher excitation requirements will have, at most, a similar size. Hence the observed main-beam brightness of the J=3–2 transition can be expressed as follows

$$T_{\text{mb}} = (1 - e^{-x^2}) T_{\text{b}}^{(\text{w})} \left(1 + \frac{e^{-x^2}}{1 - e^{-x^2}} C \right) \quad (2)$$

where $T_{\text{b}}^{(\text{w})}$ is the brightness temperature of the warm gas in the nucleus, $x = \sqrt{\ln 2} d / \Theta_{\text{HPBW}}$ (a disk source assumed), and $C = T_{\text{r}}^{(\text{c})} / T_{\text{r}}^{(\text{w})}$ is the ratio of radiation temperatures for J=3–2 of the cold and warm gas phase. The former dominates at larger galactocentric distances in this galaxy (Papadopoulos & Seaquist 1998), and fills the rest of the $14''$ beam.

Substituting $d = 8''$ and $\Theta_{\text{HPBW}} = 14''$ we obtain $T_{\text{b}}^{(\text{w})} = 4.94 (1 + 3.94C)^{-1} T_{\text{mb}}$, which we plot in Figure 3 (for $C = 0$) together with the ^{12}CO J=1–0 brightness temperature averaged over the inner diameter of $\sim 8''$.

EDITOR: PLACE FIGURE 3 HERE.

The excellent agreement between the two spectral line profiles demonstrates that they arise from the same region, which the high-resolution ^{12}CO J=1–0 maps (e.g. Tacconi & Genzel 1996) allow us to identify with the inner $8''$. The velocity-averaged $R_{32} = (3 - 2)/(1 - 0)$ ratio for that region is $R_{32} \sim 1.1$ ($C=0$). If the typical physical characteristics of the cold phase, namely $n(\text{H}_2) \approx 3 \times 10^2 \text{ cm}^{-3}$ and $T_{\text{kin}} \approx 10 \text{ K}$ (Papadopoulos & Seaquist 1998), dominate beyond the central $8''$ while warm and dense gas ($n(\text{H}_2) > 10^3 \text{ cm}^{-3}$, $T_{\text{kin}} > 20 \text{ K}$) is present in the central region, then $C \sim 0.030 - 0.045$. This yields a range $R_{32} \sim 0.95 - 1.0$, which for a gaussian source brightness will be somewhat lower, namely $\sim 0.80 - 0.85$.

Such high R_{32} ratios are characteristic of an optically thick and thermalised J=3–2 transition at gas temperatures of $T_{\text{kin}} \gtrsim 30 \text{ K}$, consistent with the deduced dust temperature of $\sim 35 \text{ K}$. A simple Large Velocity Gradient (LVG) analysis (e.g. Richardson 1985) yields a variety of conditions that can produce $R_{32} \sim 0.8 - 1.1$, all of them characterized by $T_{\text{kin}} \gtrsim 30 \text{ K}$ and with the most typical temperature being $\sim 50 \text{ K}$. This suggests that most of the molecular ISM in the starburst nucleus of NGC 7469 is indeed warm with its dust emission dominating the global mm/sub-mm/FIR spectrum (Figure 2).

4. Discussion

The high R_{32} ratio and gas temperature inferred for the central region of NGC 7469 are in sharp contrast with the low $R_{21} = (2 - 1)/(1 - 0) \sim 0.5$ and $T_{\text{kin}} \approx 10 \text{ K}$ characterizing the global CO emission from its disk (Papadopoulos & Seaquist 1998). Such steep excitation gradients in spiral galaxies, particularly the ones with starburst nuclei, are expected and known to exist in numerous cases (Knapp et al 1980; Wall & Jaffe 1990; Wall et al. 1991; Eckart et al 1991; Harris et al. 1991; Wild et al. 1992; Aalto et al. 1995). This is further corroborated by the new generation of mm and sub-mm bolometers that allow sensitive

imaging of the dust emission out to large galactocentric distances and show large masses of cold dust ($T_d = 10 - 15$ K) residing in spiral disks away from the nucleus (e.g. Neininger et al. 1996; Dumke et al. 1997; Alton et al. 1998; Papadopoulos & Seaquist 1999a).

It is often argued that such a cold dust component is responsible for a systematic underestimate of dust mass when only FIR data are used. This would naturally lead to the large $M(H_2)/M_d \sim 500 - 600$ ratios ($M(H_2 + HI) \sim 1000$ when HI is included) found for spiral galaxies in contrast to $\sim 100 - 150$ found for the Milky Way (e.g. Devereux & Young 1990 and references therein). On the other hand extragalactic $M(H_2)$ estimates are thought to be accurate to within a factor of ~ 2 (Young & Scoville 1991), and particularly for spirals to within $\pm 30\%$ (Devereux & Young 1990). However recent sensitive sub-mm imaging at $450 \mu m$ and $850 \mu m$ of IR-bright spirals like NGC 891 (Alton et al. 1998) and NGC 1068 (Papadopoulos & Seaquist 1999a) reveals that the warm and cold dust are spatially well separated, with the former being concentrated mainly in the inner $\lesssim 2$ kpc where significant star formation occurs and the latter residing at larger galactocentric radii.

The case of NGC 1068 is particularly relevant since its host galaxy properties are remarkably similar to NGC 7469 (Wilson et al. 1991), with both galaxies harboring a central starburst and having similar FIR, ^{12}CO J=1–0 and HI luminosities. The relative proximity of NGC 1068 allowed extensive multi-line CO and sub-mm imaging of its inner 2.5 kpc (Papadopoulos & Seaquist 1999a, 1999b) which showed that the bulk of the gas and dust in that region is warm with $M(H_2)/M_d \sim 330$. The latter is essentially identical to the total gas-to-dust ratio since most of the gas in the circumnuclear starburst of NGC 1068 is molecular. This ratio is actually $\sim 30 - 40\%$ higher still if the bright ^{12}CO J=3–2 emission is subtracted from the $850 \mu m$ flux used to estimate the dust mass. In the regions beyond the starburst nucleus of NGC 1068 emission from cold dust ($T_d \sim 10 - 15$ K) dominates the sub-mm bands, while low-brightness ^{12}CO J=1–0 and bright HI emission reveal the diffuse

H₂ and HI that make up the gas reservoir (Papadopoulos & Seaquist 1999a). Interestingly the total gas-to-dust ratio in those regions is $\sim 70 - 150$, close to the Galactic value.

The larger distance of NGC 7469 precludes a similar detailed study, however the high-resolution ¹²CO J=1–0 and 450 μ m maps (Figure 1) together with the lower limit of ~ 35 K for the dust/gas temperature in its central 8'' allow for a firm lower limit on the gas-to-dust ratio in that region. We measure $S_{450}(r \leq 4'') = (0.80 \pm 0.08)$ Jy, probably a slight overestimate owing to the larger beam area at this wavelength coupling to a region somewhat larger than the inner 8'', beyond which only faint sub-mm emission from cold dust is expected. The velocity-integrated ¹²CO J=1–0 line flux is $S_{CO}(r \leq 4'') = (175 \pm 25)$ Jy km s^{−1}, estimated from the original high resolution map. Assuming that H₂ dominates the gas phase in the starburst region, a Galactic X_{CO}, and T_d = 35 K, yields a total gas-to-dust ratio of ~ 500 .

Hence for both NGC 7469 and NGC 1068 it can be convincingly argued that the high gas-to-dust ratios found for their IR-luminous starbursting central regions are not due to the presence of significant amounts of cold dust but to an overestimate of the molecular gas mass in such environments. In the case of NGC 7469 this conclusion is further supported by a dynamical study of its central region concluding that X_{CO} is $\sim 1/5$ of the Galactic value (Genzel et al. 1995). This would bring the gas-to-dust ratio estimated for that region in good accord with the Milky Way value with no need for an unaccounted mass of cold dust.

4.1. The systematic overestimate of M(H₂) in starburst environments

There has been mounting evidence that the Galactic value of X_{CO} overestimates the molecular gas mass in the intense starburst environments of luminous IR galaxies ($L_{FIR} > 10^{11} L_{\odot}$ by a factor of ~ 5 (Solomon et al. 1997; Downes & Solomon 1998). This

seems to be due to a two-phase differentiation that the molecular gas undergoes in such environments (Aalto et al. 1995; Downes & Solomon 1998). The phase that dominates the ^{12}CO emission is diffuse, warm and possibly non self-gravitating, the latter being the main reason for the overestimate of molecular gas when a Galactic value for X_{CO} is used.

Indeed a standard expression for this conversion factor is (e.g. Bryant & Scoville 1996)

$$X_{\text{CO}} = 2.1 \frac{n^{1/2}}{T_b} Q M_{\odot} (\text{K km s}^{-1})^{-1} \quad (3)$$

where n (cm^{-3}) is the average gas density and T_b (K) is the average brightness temperature of ^{12}CO J=1–0 of the molecular cloud ensemble. The factor $Q = \delta V_{\text{vir}}/\delta V$ accounts for the non-virial linewidth of the “average” cloud, for self gravitating clouds it is $Q = 1$.

For typical conditions in the Galaxy, namely $Q \approx 1$, $n \approx 300 \text{ cm}^{-3}$ and $T_{\text{kin}} \approx 15 \text{ K}$ ($T_b \approx 8 \text{ K}$), one obtains $X_{\text{CO}} \approx 5 M_{\odot} (\text{K km s}^{-1})^{-1}$, the typical Galactic value. In the diffuse molecular phase that is present in starburst nuclei, it can be $Q < 1$ (e.g. Solomon et al. 1997), thus a Galactic X_{CO} will overestimate the molecular gas mass present. Moreover, even in the case of self-gravitating clouds, a diffuse ($n \approx 10^3 \text{ cm}^{-3}$) but warm phase ($T_{\text{kin}} \sim 60 \text{ K}$) dominating the ^{12}CO J=1–0 emission will have $T_b = 30 - 40 \text{ K}$ ($\tau_{10} \sim 2 - 4$) and thus yield a X_{CO} factor that is $\sim 2 - 3$ times smaller than the Galactic value.

If such a gas phase is characteristic of the starburst regions in luminous IR galaxies, then a *systematic* overestimate of H_2 mass rather than an underestimate of dust mass is responsible for the high $M(\text{H}_2)/M_d$ ratios found for them. Because the effect is systematic it can produce both a high total gas-to-dust ratio and a small dispersion around its mean. Hence earlier claims that such small dispersion ($\sim \pm 30\%$) observed in IR-luminous spirals (Devereux & Young 1990) argues in favor of a similar accuracy in molecular gas mass estimates are not supported by this picture.

4.2. The cold gas and dust in NGC 7469

The global excitation of CO in NGC 7469 seems to be dominated by cold and diffuse molecular gas out to a scale of $d \lesssim 20''$ (Papadopoulos & Seaquist 1998). A gaussian fit of the $850 \mu\text{m}$ emission (Figure 1) yields a source size of $\sim 17.2'' \times 18.5''$ (FWHM), clearly larger than the beam at this wavelength. Considering the geometric mean of $\Theta_s \sim 18''$ to be the observed diameter of the source (assumed to be a disk), and for a gaussian beam with $\Theta_{\text{HPBW}} = 15''$, we obtain an intrinsic source diameter of $d = [2 (\ln 2)^{-1} (\Theta_s^2 - \Theta_{\text{HPBW}}^2)]^{1/2} \sim 17''$. This is ~ 2 times larger than the size of the bright $^{12}\text{CO J=1-0}$ emission and comparable to the source size seen at $450 \mu\text{m}$ (Figure 1).

In NGC 1068 the warm gas/dust resides in the inner $d \sim (2.7 - 3.4)$ kpc, which is comparable to the size of a similar region in NGC 7469, both regions containing an embedded starburst. Furthermore, given the similarities of the disk properties between these two galaxies, it is reasonable to identify the extended faint sub-mm, $^{12}\text{CO J=1-0}$ emission in NGC 7469 with emission from cold dust/gas. Indeed simply scaling the total size of the faint sub-mm emission from cold dust in NGC 1068 (~ 6 kpc) to the distance of NGC 7469 yields an angular size of $\sim 20''$, closely matching the one observed for the latter.

It is intriguing that faint $^{12}\text{CO J=1-0}$ emission is detected out to significantly larger radii than the inner radius of $r = 4''$ (Figure 1). Assuming that, as in NGC 1068, this emission “marks” cold and diffuse H_2 coexisting with cold dust ($T_d = 10 - 15$ K) and the bulk of HI, yields a ratio $[M(\text{H}_2 + \text{HI})]/M_d \sim 50 - 160$, close to the Milky Way value.

4.3. Warm versus cold gas/dust: sub-mm imaging and CO spectroscopy

It is striking that in the spatially integrated dust emission of this galaxy the cold dust is inconspicuous even after the inclusion of the sub-mm data. On the other hand its

molecular gas counterpart dominates the global excitation characteristics as revealed by the low ^{12}CO ($J=2-1$)/($J=1-0$) line ratio (Papadopoulos & Seaquist 1998).

This could simply be due to the fact that spectral line luminosity is sensitive to the local gas density as well as its temperature and total mass but only the latter two determine the continuum luminosity from dust (for a fixed gas-to-dust ratio). In other words two molecular clouds with the same mass and gas/dust temperature will emit the same dust continuum (optically thin case) but their CO line fluxes can differ drastically if their average H_2 densities are different. This will occur mainly in the density regime of sub-thermal excitation of the observed CO line(s).

In NGC 7469 the relative amounts of warm and cold dust can be estimated from the relation

$$m = \frac{M_d^{(c)}}{M_d^{(w)}} = \left[\frac{e^{32/T_c} - 1}{e^{32/T_w} - 1} \right] \frac{S_{450}^{(c)}}{S_{450}^{(w)}}, \quad (4)$$

where (w) and (c) denote the quantities corresponding to the warm and cold dust respectively. It is $S_{450}^{(w)} = S_{450}(r \leq 4'') = 0.8 \text{ Jy}$ and $S_{450}^{(c)} = S_{450}(4'' \leq r \leq 11'') = 0.5 \text{ Jy}$. Hence for $T_w \gtrsim 35 \text{ K}$ and $T_c = 10 - 15 \text{ K}$ we obtain $m \gtrsim 3 - 10$.

Even for $m \sim 10$, the spatially averaged sub-mm emission will not necessarily reveal the presence of the cold component. Indeed, since the ratio $r = S_{450}/S_{850}$ is temperature-sensitive when $T_d \lesssim 30 \text{ K}$, it is expected to differ if a cold dust component is present along with the warm one. Assuming spatial averaging of the emission from the two dust components the observed r can be written as follows

$$r = r_w \left[\frac{1 + m f_{450}(T_w, T_c)}{1 + m f_{850}(T_w, T_c)} \right], \quad (5)$$

where r_w is the ratio corresponding to warm dust alone and,

$$f_{\lambda}(T_w, T_c) = \frac{e^{T_{\lambda}/T_w} - 1}{e^{T_{\lambda}/T_c} - 1}, \quad T_{\lambda} = \frac{h \, c}{\lambda \, k}. \quad (6)$$

For $T_w = 40$ K, $T_c = 10$ K and $m = 10$ we obtain $r \approx 0.70 \times r_w$, which is barely discernible from r_w given that the value of r carries a $\sim 20\%$ uncertainty due to the calibration uncertainties of SCUBA at $450 \, \mu\text{m}$ and $850 \, \mu\text{m}$.

On the other hand besides temperature the spectral line ratios are also sensitive to the local gas density. Thus a cold *and sub-thermally excited* molecular gas phase may dominate the observed global line ratio even in the presence of a warm and thermalized phase. For example, the global $R_{21} = (2 - 1)/(1 - 0)$ ratio can be expressed as

$$R_{21} = R_{21}^{(w)} \left[\frac{1 + m \, x \, (R_{21}^{(c)}/R_{21}^{(w)})}{1 + m \, x} \right], \quad (7)$$

where $x = X_{\text{CO}}^{(w)}/X_{\text{CO}}^{(c)}$ is the ratio of the CO(1–0)-to-H₂ conversion factors for the two gas phases. Assuming $x \sim 1/5$, $m \sim 10$ and, $R_{21}^{(w)} \sim 1$, we obtain $R_{21} \sim 1/3 \, (1 + 2 \, R_{21}^{(c)})$.

In NGC 7469 it is $R_{21} \approx 0.5$ (Papadopoulos & Seaquist 1998), hence the cold-phase ratio will be $R_{21}^{(c)} \approx 0.25$, and for $T_{\text{kin}} = 10$ K, the latter corresponds to densities of $n(\text{H}_2) \approx 10^2 \, \text{cm}^{-3}$. For the same temperature but thermalized and optically thick ¹²CO J=2–1 it is $R_{21}^{(c)} \approx 0.8$, yielding $R_{21} \approx 0.85$ which is significantly larger than observed.

The aforementioned simple analysis demonstrates the significance of combining sub-mm and CO observations in evaluating the physical conditions and the mass of molecular gas. The sub-mm measurements offer an independent means of estimating gas mass under the assumption of a canonical gas-to-dust ratio of ~ 100 . For H₂-dominated gas this mass can then be compared to the one deduced from the ¹²CO J=1–0 luminosity and the X_{CO} conversion factor and hence the influence of the physical conditions on X_{CO} can be assessed. On the other hand, if a cold and diffuse molecular gas phase is present along with a warm

one but only global averages are available, CO line ratios can be more sensitive to the presence of the cold ISM phase than sub-mm intensity ratios.

5. Conclusions

We presented sensitive 850 μm , 450 μm maps of the Seyfert 1 galaxy NGC 7469 and a measurement of the ^{12}CO J=3–2 line towards its starbursting central region. Our main conclusions can be summarized as follows

1. The FIR/sub-mm/mm spectrum of this source is dominated by a warm dust component with a temperature of ~ 35 K and a global molecular gas-to-dust ratio of ~ 600 , both typical for IR-luminous spirals. Including the atomic gas mass yields a total gas-to-dust ratio of ~ 800 .

2. The warm dust and gas lies in the inner $8''$ (~ 2.5 kpc) where a starburst is embedded. In this region we find no evidence for a significant mass of cold dust, yet the ratio of the mainly molecular gas to the dust mass is ~ 500 , still five times larger than the Galactic value. We argue that this is the result of a systematic overestimate of H_2 mass by a factor of ~ 5 when a Galactic value for $X_{\text{CO}} = \text{M}(\text{H}_2)/\text{L}_{\text{CO}}$ is used in starburst environments.

3. On larger scales (radius $\gtrsim 1.2$ kpc) the ISM in NGC 7469 is dominated by cold, sub-thermally excited gas where the faint 450 μm and ^{12}CO J=1–0 emission originate. The gas-to-dust ratio for this phase, is $\sim 50 - 150$; in better accord with the Milky Way value.

5.1. Acknowledgments

We would like to thank Linda Tacconi for providing us with data prior to publication, Henry Matthews for obtaining the SCUBA maps, and Remo Tilanus for conducting the CO observations on our behalf. P. P. Papadopoulos is supported by the “Surveys with the Infrared Space Observatory” network set up by the European Commission under contract FMRX-CT96-0086 of its TMR programme.

A. Spectral line contribution to mm/sub-mm bands

In mm and sub-mm continuum observations one must correct for non-dust emission contributions. The most significant comes from molecular spectral lines and can reach up to $\sim 60\%$ of the total flux observed with a typical bolometer bandwidth (Gordon 1995). In warm cores of Orion such line contributions are found to be of the order of $\sim 30\%$ in 850 μm and 450 μm bands (Johnstone & Bally 1999 and references therein). However in the extragalactic domain a typical beam of a mm/sub-mm telescope samples areas of several hundred parsecs, and the contributions from warm cores (≤ 1 pc) in star forming regions are negligible because of the resulting spatial dilution. Over such scales only the emission from the three lowest rotational transitions of ^{12}CO can be ubiquitous and bright, since these transitions can be easily excited in the general conditions prevailing in the ISM in quiescent or starburst environments.

In the case of NGC 7469 we expect that all the significant spectral line emission from the ^{12}CO J=2–1 (1.3 mm band) and ^{12}CO J=3–2 (850 μm band) lines arises from the region of bright ^{12}CO J=1–0 emission in the central $8''$ where the starburst resides. In the case of the 1.3 mm band only line-free channels were used to produce the continuum map (Tacconi, private communication). The 850 μm band includes the ^{12}CO J=3–2 line whose contribution can be estimated from our observation of this line towards the nucleus, namely

$$S_{850}^{(\text{dust})} = S_{850} - \frac{2 k \nu_o^3}{c^3 \Delta\nu_B} \left(\frac{x^2}{1 - e^{-x^2}} \right) I_{\text{mb}} \Omega_{\text{mb}} \quad (\text{A1})$$

where I_{mb} (K km s^{-1}) is the velocity-integrated main-beam brightness of ^{12}CO J=3–2, $\nu_o = 345.796$ GHz, and Ω_{mb} is the gaussian beam area at this frequency. The term in the parenthesis corrects for the beam-source geometrical coupling assuming a disk source of diameter d , where $x = \sqrt{\ln 2} d / \Theta_{\text{HPBW}}$, and $\Delta\nu_B$ is the bolometer bandwidth.

For ^{12}CO J=3–2 in NGC 7469 we measured $I_{\text{mb}} = (77 \pm 8) \text{ K km s}^{-1}$ (Figure 3), hence for $\Theta_{\text{HPBW}} = 14''$, $\Delta\nu_{\text{B}} = 30 \text{ GHz}$ (Holland, private communication) and $d = 8''$ we obtain a line contribution of $\Delta S = 63 \text{ mJy}$, which amounts to $\sim 40\%$ of the total flux at $850 \mu\text{m}$. The ^{13}CO J=3–2 is expected to have $\lesssim 0.1$ of the ^{12}CO J=3–2 flux, and hence contribute $\lesssim 4\%$ of the total flux in $850 \mu\text{m}$.

In the case of the $450 \mu\text{m}$ band the only CO line that may contribute to the observed flux is ^{13}CO J=6–5 at 661.067 GHz . However we find that this line, with its high excitation density ($n > 10^5 \text{ cm}^{-3}$), will not contribute significantly to the $450 \mu\text{m}$ band (i.e. $\lesssim 2\%$) over the spatial scales relevant here, even in a starburst environment.

REFERENCES

- Aalto, S., Booth, R. S., Black, J. H., & Johansson, L. E. B. 1995, *A&A*, 300, 369
- Alton, P. B., Bianchi, S., Rand, R. J., Xilouris, E. M., Davies, J. I., & Trewhella, M. 1998, *ApJ*, 507, L125
- Bryant, P. M., & Scoville, N. Z. 1996, *ApJ*, 457, 678
- Cutri, R. M., Rudy, R. J., Rieke, G. H., Tokunaga, A. T., & Willner, S. P. 1984, *ApJ*, 280, 521
- Devereux, N. A., & Young, J. S. 1990, *ApJ*, 359, 42
- Downes, D., Solomon, P. M. 1998, *ApJ*, 507, 615
- Dumke, M., Braine, J., Krause, M., Zylka, R., Wielebinski, R., & Guélin M. 1997, *A&A*, 325, 124
- Eckart, A., Cameron, M., Jackson, J. M., Genzel, R., Harris, A. I., Wild, W., & Zinnecker, H. 1991 *ApJ*, 372, 67
- Genzel, R., Weitzel, L. E., Tacconi-Garman, L. E., Blietz, M., Cameron, M., Krabbe, A., & Lutz, D. 1995, *ApJ*, 444, 129
- Gordon, M. A. 1995, *A&A*, 301, 853
- Harris, A. I., Hills, R. E., Stutzki, J., Graf, U. U., Russel, A. P. G., & Genzel, R. 1991, *ApJ*, 382, L75
- Hildebrand, R. H. 1983, *MNRAS*, 24, 267
- Holland. W. S., Robson, E. I., Gear, W. K., Cunningham, C. R., Lightfoot, J. F., Jenness, T., Ivison, R. J., Stevens, J. A., Ade, P. A. R., Griffin, M. J., Duncan W. D., Murphy J. A., & Naylor, D. A. 1998 *MNRAS*, 303, 659

- Knapp, G. R., Phillips, T. G., Huggins, P. J., Leighton, R. B., & Wannier, P. G. 1980 ApJ, 240, 60
- Jenness, T., & Lightfoot, J. F. 1998 in SURF-SCUBA User Reduction Facility, User’s manual
- Jenness, T., Lightfoot, J. F., & Holland, W. S. 1998, astro-ph/9809120
- Johnstone, D., & Bally, J. 1999, ApJ, 510, L49
- Krolik, J. H. in “The Interstellar Medium in Galaxies”, pg 239, Kluwer Academic Publishers, H. A. Thronson Jr., & J. M. Shull (Eds)
- Israel, F. P. 1997, A&A, 328, 471
- Matthews, H. in “Receiver B3 User Information”, 1999, (<http://www.jach.hawaii.edu/JACpublic/JCMT/>)
- Meixner, M., Puchalsky, R., Blitz, L., Wright, M., & Heckman, T. 1990, ApJ, 354, 158
- Miller, J., & Antonucci, R. 1983, ApJ, 271, L7
- Mirabel I. F., & Wilson A. S. 1984, ApJ, 277, 22
- Neininger, N., Guélin, M., García-Burillo, S., Zylka, R., & Wielebinski, R. 1996 A&A, 310, 725
- Papadopoulos, P. P., & Seaquist, E. R. 1998, ApJ, 492, 521
- Papadopoulos, P. P., & Seaquist, E. R. 1999a, ApJ, 514, L95
- Papadopoulos, P. P. & Seaquist, E. R. 1999b, ApJ, 516, 114
- Soifer, B. T., Boehmer, L., Neugebauer, G., & Sanders, D. B. 1989, AJ, 98, 766

- Sandell, G. 1998, The SCUBA mapping cookbook, A first step to proper map reduction.
- Solomon, P. M., & Barrett J. W. 1991, in IAU Symp. 146, Dynamics of Galaxies and Molecular Cloud Distribution (Dordrecht: Kluwer), 235
- Solomon, P. M., Downes, D., Radford, S. J. E., & Barrett, J. W. 1997, ApJ, 478, 144
- Stark, A. A., Knapp, G. R., Bally, J., Wilson, R. W., Penzias, A. A., & Rowe, H. E. 1986, ApJ, 310, 660
- Tacconi, L. J., & Genzel, R. 1996 in “Science with Large Millimetre Arrays”, pg. 125, ESO Astrophysics Symposia, Springer (Ed. P. A. Shaver)
- Tacconi, L. J., Genzel, R., Gallimore, J. & Tacconi-Garman L. E. 2000, ApJ, (in press)
- Richardson, K. J. 1985, PhD thesis, Department of Physics, Queen Mary College, University of London
- Wall, W. F., & Jaffe, D. T. 1990 ApJ, 361, L45
- Wall, W. F., Jaffe, D. T., Israel, F. P., & Bash, F. N. 1991 ApJ, 380, 384
- Wild, W., Harris, A. I., Eckart, A., Genzel, R., Graf, U. U., Jackson, J. M., Russell, A. P. G., & Stutzki, J. 1992, A&A, 265, 447
- Wilson, A. S., Helfer, T. T., Haniff, C. A., & Ward, M. J. 1991, ApJ, 381, 79
- Young, J. S., Schloerb, F. P., Kenney, J. D., & Lord, S. D. 1986, ApJ, 304, 443
- Young, J. S., Xie, S., Kenney, J. D., & Rice, W. L. 1989, ApJS, 70, 699
- Young, J. S., & Scoville, N. Z. 1991 ARA&A, 29, 581

Fig. 1.— Top: the 850 μm map with a FWHM= 15'' beam shown at the lower left, the contours are $(-3, 3, 6, 9, 12, 15, 18, 21, 24, 27, 30) \times \sigma_{850}$, with $\sigma_{850} = 5 \text{ mJy beam}^{-1}$.

Bottom: the 450 μm map (contours) overlaid to the integrated ^{12}CO J=1–0 emission (grey scale) at a common resolution of 9'' (FWHM beam shown at the bottom left). The contours are $(-4, 4, 6, 8, 10, 14, 16, 18) \times \sigma_{450}$, with $\sigma_{450} = 40 \text{ mJy beam}^{-1}$ and the grey scale is $I=6\text{--}200 \text{ Jy beam}^{-1} \text{ km s}^{-1}$ ($\sigma(I) = 1 \text{ Jy beam}^{-1} \text{ km s}^{-1}$)

The map center is at RA: 23^h 03^m 15^s.6, Dec: +08° 52' 26'' (J2000).

Fig. 2.— A χ^2 -fitted SED for the mm/sub-mm/FIR data of NGC 7469 (Table 1). An optically thin isothermal dust reservoir has been assumed with an emissivity law of $\alpha = 2$ and emissivity at 200 μm (1196 GHz) of $k_o = 10 \text{ cm}^2 \text{ gr}^{-1}$ (Hildebrand 1983). The flux at 25 μm is not used in the fit.

Fig. 3.— The ^{12}CO J=1–0 and J=3–2 brightness temperatures for the inner 8'' of NGC 7469 (see text). The thermal rms uncertainty across the band is $\delta T_{\text{rms}}(1 - 0) = 30 \text{ mK}$, and $\delta T_{\text{rms}}(3 - 2) = 40 \text{ mK}$.

Table 1

NGC 7469: The mm, sub-mm and FIR data

Wavelength	Flux	Reference
1.3 mm	19 ± 5 mJy	Tacconi et al. 1999 ^a
850 μ m	91 ± 13 mJy	this work ^b
450 μ m	1.30 ± 0.14 Jy	this work ^b
100 μ m	34.9 ± 0.6 Jy	Soifer et al. 1989
60 μ m	27.7 ± 0.04 Jy	“ “
25 μ m	5.84 ± 0.05 Jy	“ “

^a Derived from the 1.3 mm continuum map for a radius of $r = 4''$ that contains all the mm emission and corrected for non-thermal emission using the data from Wilson et al. 1991.

^b Fluxes are estimated for a radius of $r = 11''$ and the appropriate error-beam corrections (Sandell 1997) are $f_{850} = 0.80$, $f_{450} = 1.05 - 1.10$, derived from Uranus and CRL 618 maps. The 850 μ m flux has also been corrected for contribution from the ^{12}CO J=3–2 line (see Appendix). The errors reported include (besides the thermal rms errors) a $\sim 10\%$ (850 μ m) and a $\sim 15\%$ (450 μ m) calibration uncertainty.

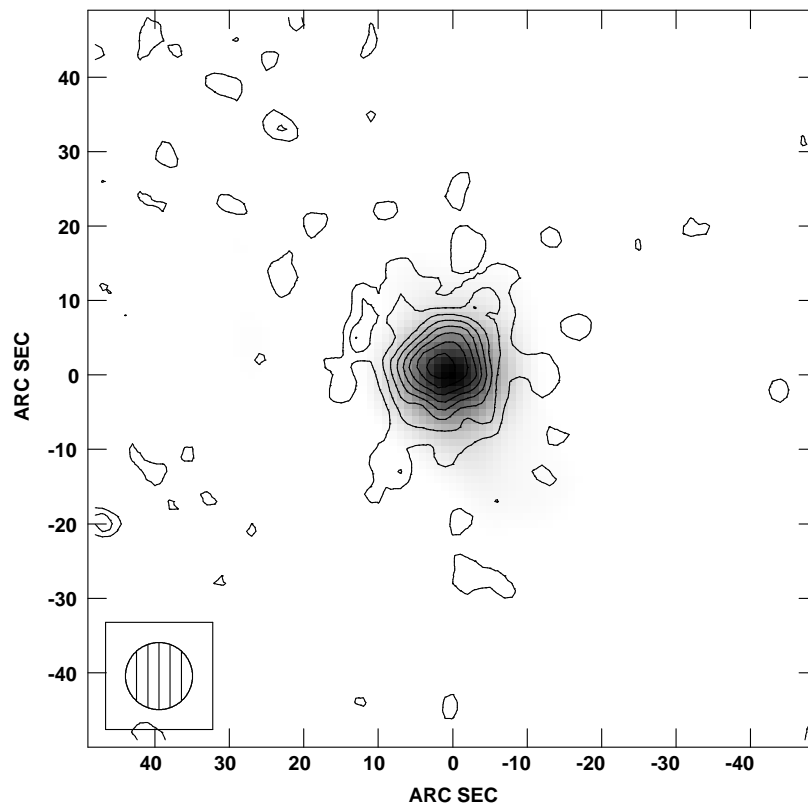
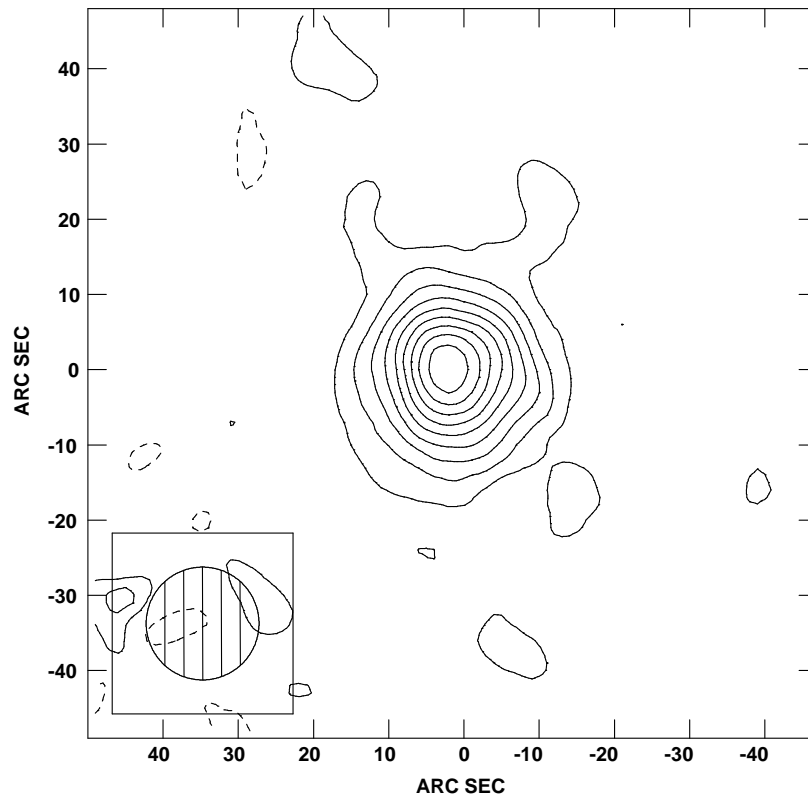
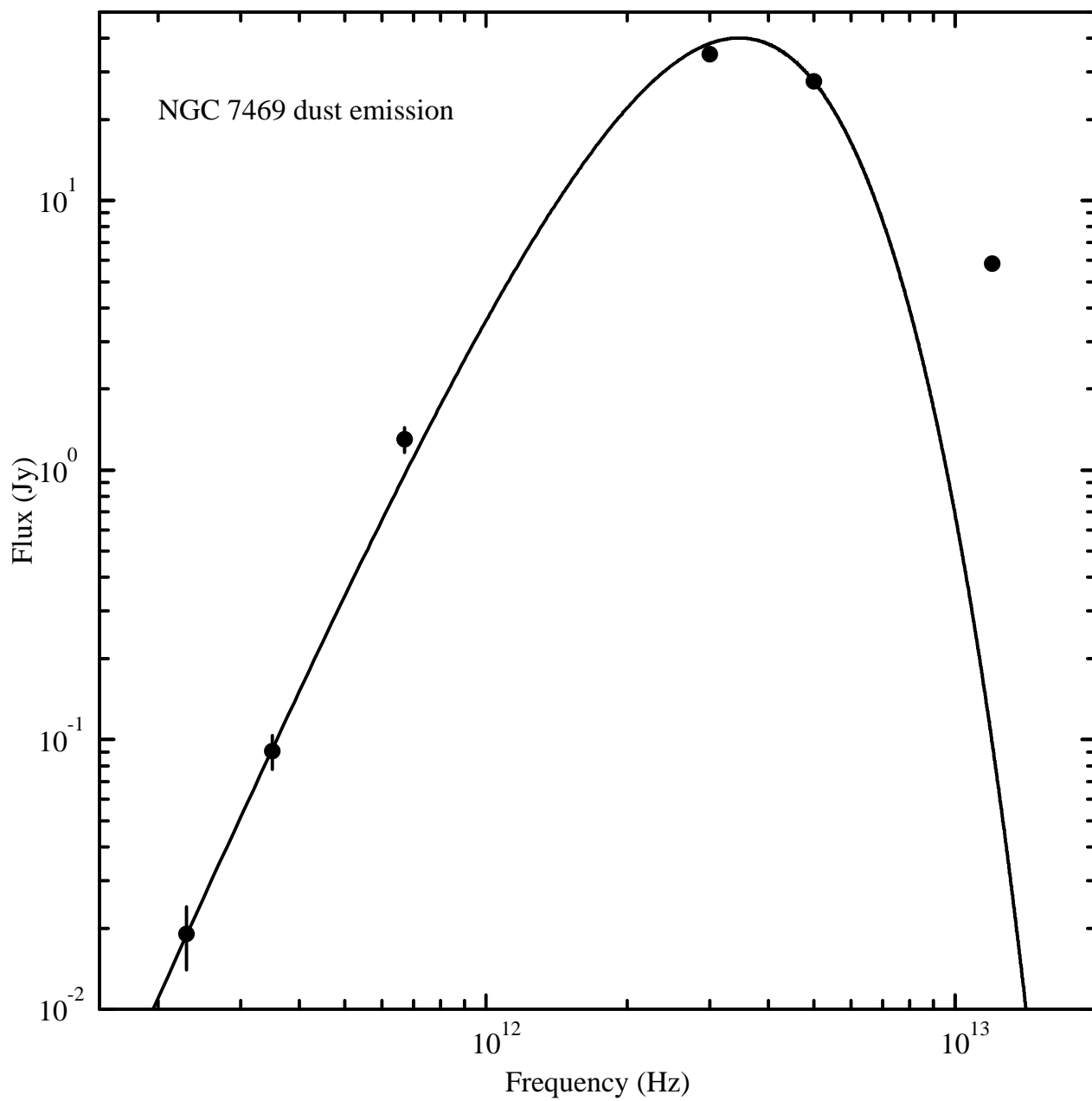


Figure 1



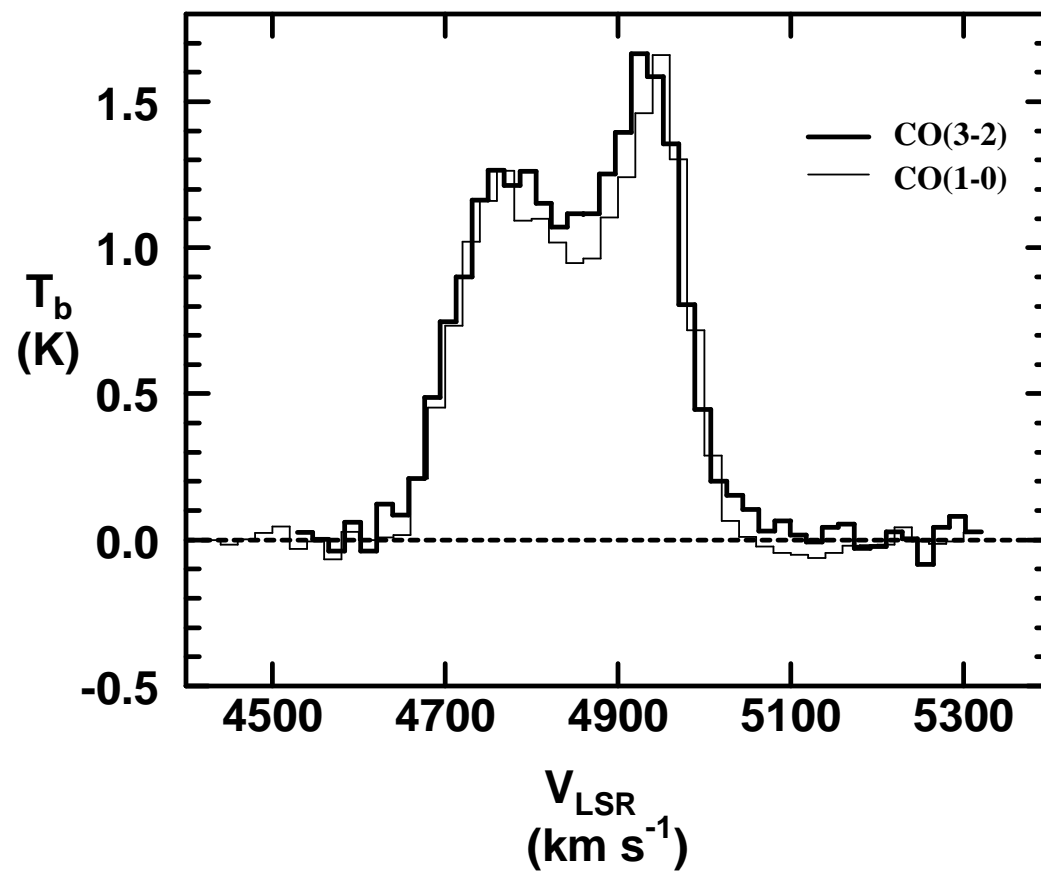


Figure 3